Journal of Petroleum
Science and Technology

Source Rock Evaluation of the Cenomanian Middle Sarvak (Ahmadi) Formation in the Iranian Sector of the Persian Gulf

Maryam Mirshahani*, Mohammad Kassaie, and Arsalan Zeinalzadeh

Geochemistry Group, Faculty of Upstream Petroleum Industry, Research Institute of Petroleum Industry (RIPI), Tehran, Iran

ABSTRACT

The middle Sarvak formation (Cenomanian) is one of the stratigraphic units of the Bangestan group in the south of Iran. This formation is stratigraphically equivalent to the Ahmadi member of Kuwait and Iraq. There is geochemical evidence that indicates this unit has a high level of organic richness and can be a possible source rock in various locations. This study focuses on the organic geochemistry of the middle Sarvak formation in the Persian Gulf region. Rock Eval pyrolysis, organic petrography, and kerogen elemental analyses were used in order to evaluate the thermal maturity and determine the kerogen type of the middle Sarvak formation. The results of this study show that middle Sarvak formation has entered the oil window in eastern and western parts of the Persian Gulf, but it is immature in the central parts. This regional pattern of organic maturation is probably a consequence of the regional uplift in the Qatar-Fars arch area. The higher maturities in the eastern and western parts are, on the other hand, attributed to its greater depth of burial. The results of the screening analyses by the Rock-Eval pyrolysis in parallel with the results of maceral and elemental analyses show that the kerogen type in the middle Sarvak formation is mainly a mixture of Types II and III.

Keywords: Middle Sarvak Formation, Rock Eval Pyrolysis, Organic Petrography, the Persian Gulf

INTRODUCTION

The Persian Gulf region is known for its prolific petroleum systems owing to the large number of active source rocks. The middle Sarvak formation is considered as a candidate source rock in the studied area based on geochemical observations. This formation is a part of the Bangestan group and is stratigraphically equivalent to the Mauddud, Ahmadi, Rumaila, and Mishrif formations of the southern Persian Gulf region [1]. The middle Sarvak formation is present throughout the Persian Gulf area. A number of geological and geochemical studies on the Sarvak formation in the south of Iran, particularly in the Zagros area, have been carried out [2-5].The goal of this study is to evaluate the source rock potential of the middle Sarvak formation in the Persian Gulf area.

Geological Setting

The Persian Gulf basin encompasses a thick sedimentary succession with alternating clastic,

***Corresponding author**

Maryam Mirshahani
Email: mirshahanim@ripi.ir
Tel: +98 21 4825 3027
Fax: +98 21 4473 9723

Article history

Received: October 31, 2015
Received in revised form: May 10, 2016
Accepted: June 19, 2016
Available online: July 22, 2017

carbonate, and evaporite sediments, which makes the area particularly prolific for hosting large hydrocarbon deposits. The oldest sediments in the area are believed to be the evaporites, shales, and dolomites of the Late-Precambrian Hormuz series [6]. Generally, there is little data about the sedimentary history of the Lower Paleozoic in the Persian Gulf region, and the sedimentary record comprises mostly of shales and sandstone with rare carbonates in the Devonian and Early Carboniferous [7]. During the Permian, carbonate shelf deposits of the Dalan formation were deposited under warm and shallow-water conditions. More arid conditions during Mid-Late Triassic formed the evaporite deposits of the Dashtak formation, which mark the end of the carbonate cycles. The middle Jurassic sediments mainly consist of normal marine organic-rich carbonates (the Surmeh formation) [8] which are capped by extensive evaporite deposits (Hith formation) of Tithonian age [9, 10]. During Cretaceous, three main stratigraphic sequences [11] were recorded in the Persian Gulf area: the Lower Cretaceous deposits of the Fahliyan, Gadvan, and Dariyan formations; the middle Cretaceous sediments comprising of the Kazhdumi and Sarvak formations; and the Upper Cretaceous deposits of the Ilam, Laffan, and Gurpi formations [12, 13]. A regional unconformity marks the end of the Cretaceous and the boundary between the Late Cretaceous and Early Tertiary sediments [14]. Orogenic folding of the adjacent Zagros during the Late Tertiary resulted in rapid uplift, extensive erosion, and the formation of a thick clastic wedge (Figure 1).

The Paleozoic structural evolution of the area generally took place along regional basement highs [15]. Recent deformation episodes, however, included a Late Cretaceous event (producing NNE-SSW trending faults) and a Late Cenozoic Zagros Orogeny event (reactivating previous folds and causing a new set of NW-SE trending folds) [16]. Apart from these events, most of the structures in the Persian Gulf basin are affected by episodic salt movements to varying extents [17].

The morphology of the Persian Gulf is highly affected by the Qatar-Fars Arc [18]. The Qatar-Fars Arc is a first-order structure that was created in the central Persian Gulf following the tectonic movements during the Late Precambrian to Early Cambrian in the region (Figure 2). It is a very large (over 100 km wide and 300 km long) regional gentle anticline [19]. According to offshore seismic data in the study area, this structure has a northeast–southwest direction in the Iranian sector of the Persian Gulf and continues southwards to the Qatar peninsula [20]. As Figure 3 demonstrates, the thicknesses of the Pabdeh, Gurpi, and Kazhdumi formations and Ahmadi member significantly decrease toward the central parts of the study area with a noticeable thinning which can be due to the effect of the Qatar-Fars Arc Paleohigh during depositional time [14].

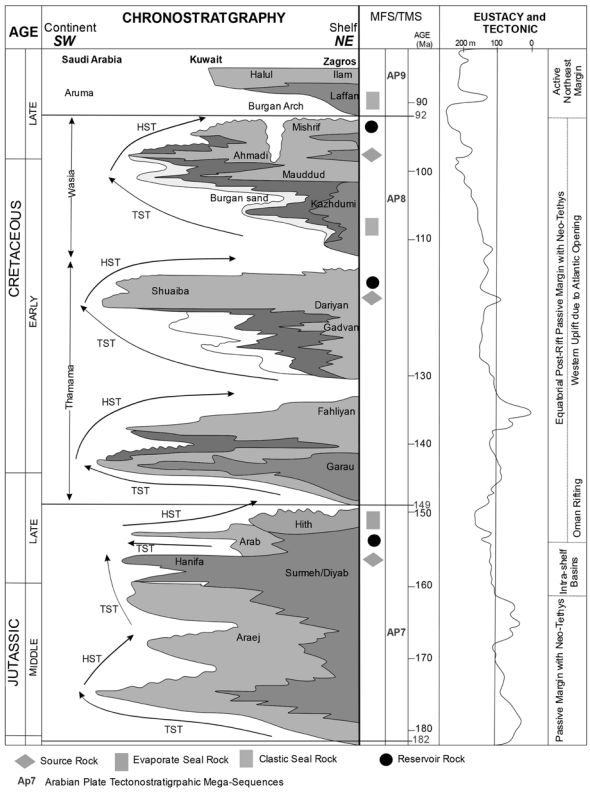

Figure 1: A generalized stratigraphic column of the study area [24].

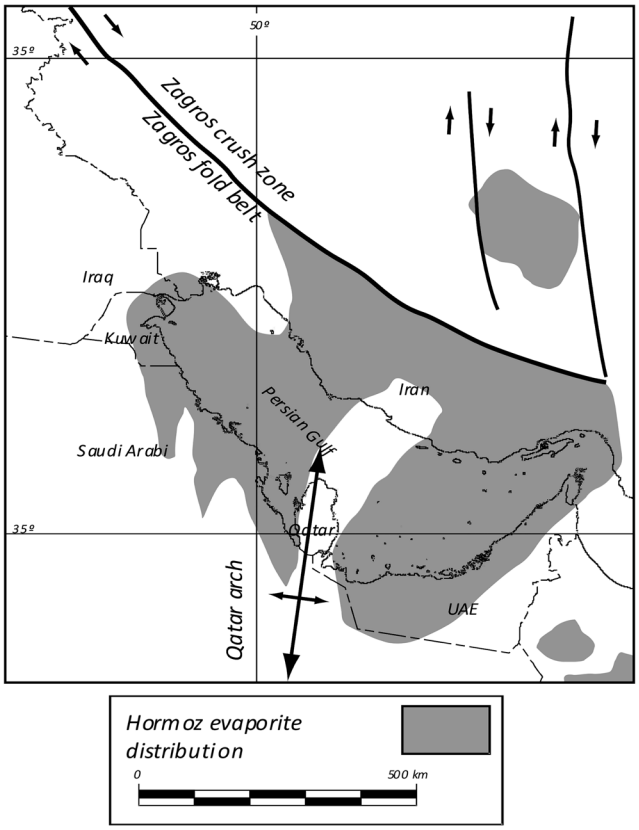

Figure 2: Location of the Qatar-Fars Arc and distribution of Hormoz Salt in the study area [21].

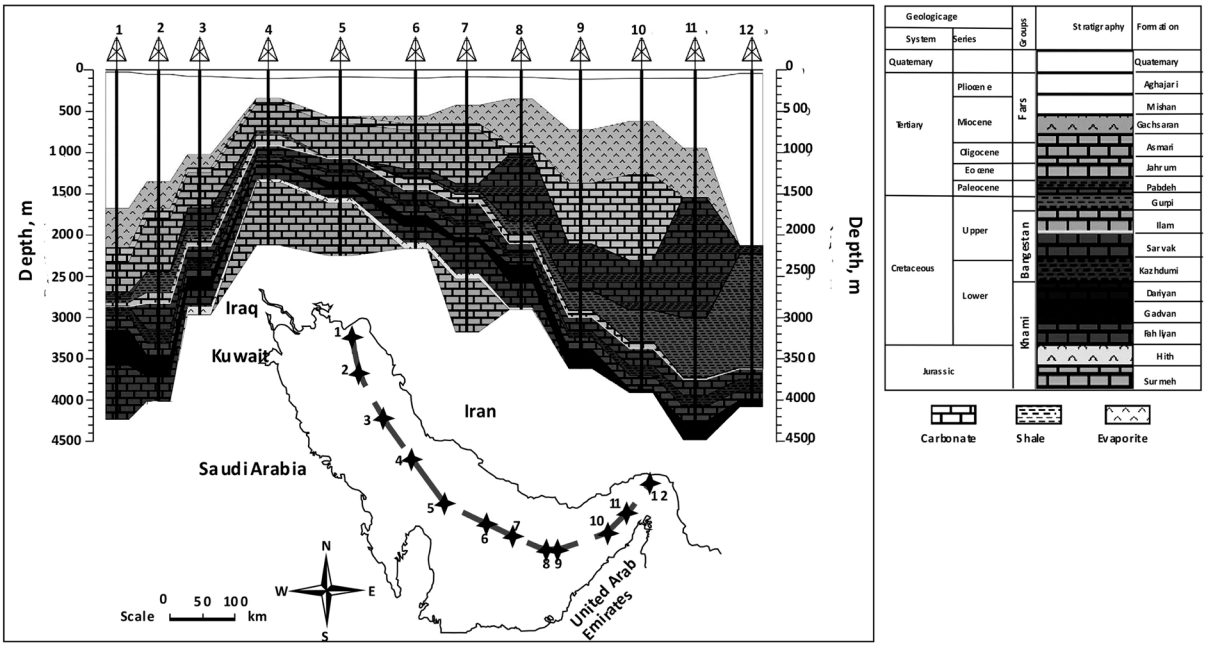

Figure 3: Lithostratigraphic cross section in the Iranian sector of the Persian Gulf through Jurassic to Quaternary (modified after [23]).

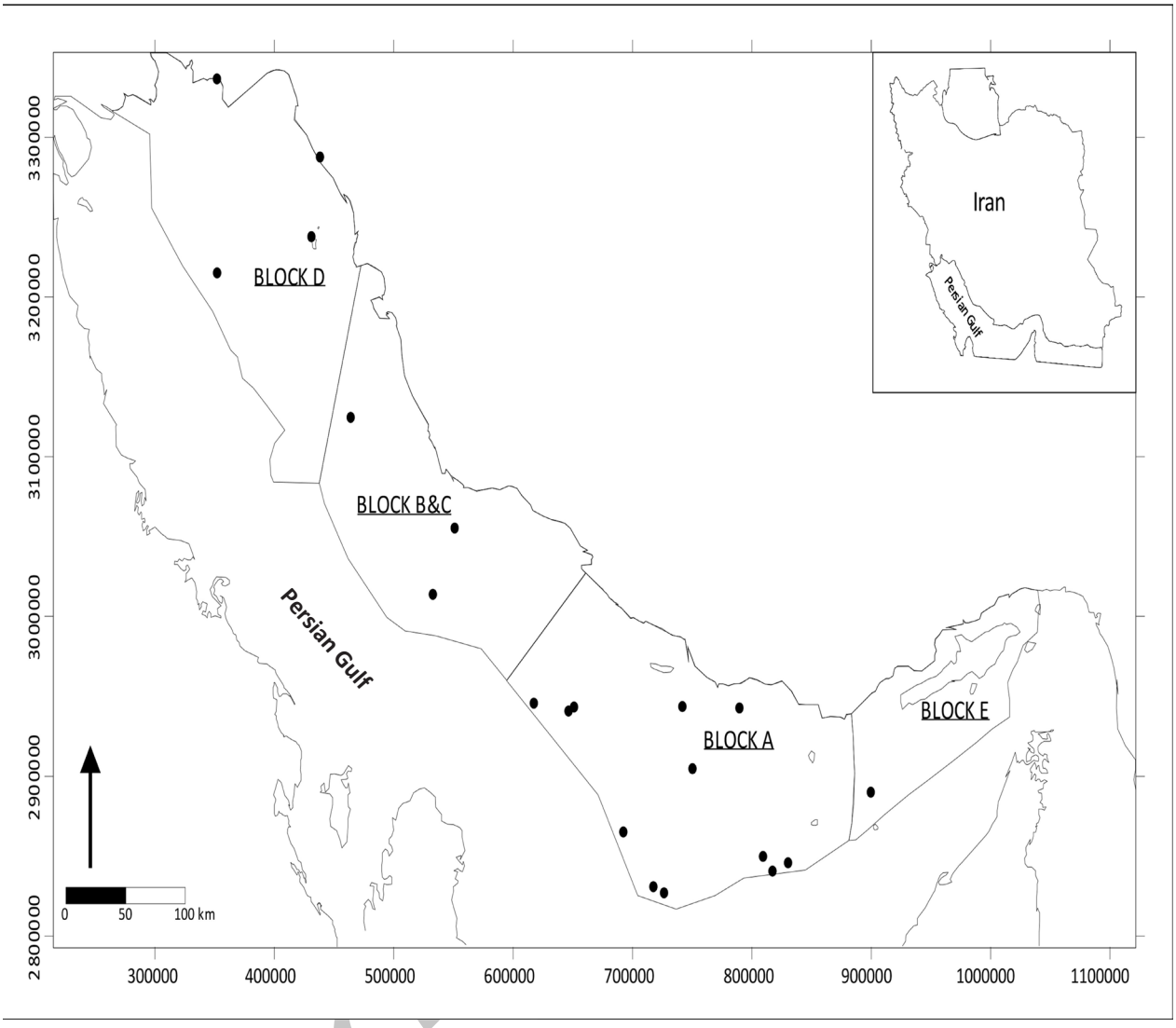

Figure 4: Location map and selected fields of the study area.

The sediments of the middle Sarvak formation were deposited on a passive margin of the Neo-Tethys Ocean. This formation is divided into four depositional members: the Mauddud, bituminous shaley limestone, Khatiyah in the central and western parts of the Persian Gulf, Ahmadi with shaley facies in the northern Persian Gulf, and the Mishrif reefal limestone [1].

The middle Sarvak is present in all wells drilled in the Persian Gulf. The thickness of the formation varies from a minimum 41 meters up to a maximum of 223 meters in the northwestern Persian Gulf [1].

The Ahmadi member is a continuation of the middle Sarvak in the northwestern Persian Gulf (towards Kuwait). Lithologically, it consists of 30 to 60 meters of highly eroded shale with intercalation of thin limestone beds. Most of the present Persian Gulf area was beyond the deltaic influence, and until the deposition of the Ahmadi shales, continued to receive sub-littoral to shallow marine carbonates [25]. The Ahmadi member also consists of fossiliferous limestones. The shale and limestone of the Ahmadi member were deposited during Early to middle Cenomanian in open-marine conditions on the outer

shelf at depths between 100 to 200 meters [1].

For the purpose of this study, in order to evaluate source rock potentiality of middle Sarvak formation, cutting samples from a total of 18 wells through the Persian Gulf area have been analyzed with organic geochemical methods. Figure 4 shows the location map of these wells in the Persian Gulf. Four study blocks were delineated to present the northwest (Block A), west-central (Block BC), east central (Block D), and east parts of the Iranian sector of the Persian Gulf.

EXPERIMENTAL PROCEDURES

Materials and Methods

In order to evaluate middle Sarvak formation for hydrocarbon source rock potentiality, Rock-Eval pyrolysis results were used in combination with organic-petrography methods. The latter included vitrinite reflectance measurements, visual kerogen inspection, thermal alteration determination, and kerogen elemental analysis following generally published procedures.

A total of 77 cutting samples were selected for analysis. Cutting cheeps were cleaned and pulverized prior to analysis. Vinci Technologies' Rock-Eval 6 instrument (AGH University of Poland) and Rock-Eval 2 unit (Research Institute of Petroleum Industry of Iran) equipped with a total organic carbon module (TOC) were used for this study.

Based on the Rock-Eval screening analyses, nine samples were selected for kerogen extraction and subsequently used for visual kerogen analyses. In order to obtain kerogen extracts, selected rock samples were crushed to an average particle size of approximately 1 mm. Concentrated HCl and HF were successively added to the pulverized cutting samples to remove carbonate and silicate materials respectively. The samples were washed in distilled water repeatedly until neutrality (pH=7) was attained, followed by the flotation of the isolated organic matter (kerogen) within zinc-bromide solution (specific gravity=2) to remove residual inorganic matter.

According to the results obtained from the screening analyses, a total of 36 samples were selected for vitrinite reflectance measurements. Vitrinite reflectance measurements were carried out on both polished whole rock block and kerogen concentrate samples by using a Leitz-MPV-SP photometer microscope at RIPI. The measurements were carried out in a random mode according to the ASTM standard method [26].

Nine polished blocks and equal number of thin sections were prepared from the extracts for the identification of kerogen type and the determination of thermal alteration index (TAI).

The kerogen extract samples were used for the elemental analyses to determine the elemental composition of C, H, N, O, and S. The elemental composition of the isolated kerogens (C, H, N, and S) was determined with a Carlo ErBa EA 1108 elemental analyzer at AGH University of Poland.

RESULTS AND DISCUSSION

Source rock characteristics of the middle Sarvak formation were performed based on a geochemical combination. Special emphasizing was on determining the type, amount, maturity, and generative potential of the contained organic matter.

Source Rock Potentiality

The results of Rock-Eval screening analyses are presented in Table 1.

Table 1: Results of Rock-Eval analyses for middle Sarvak formation.

Block	Well	Depth(m)	TOC	T_{MAX}(°C)	S1	S1/TOC	S2	S3	PI	HI	OI
A	1	1805	1.93	416	1.30	0.67	10.12	1.24	0.11	524	64
		1509	0.54	424	0.53	0.98	1.96	1.88	0.21	363	348
	2	1329	0.17	434	0.07	0.41	0.16	0.70	0.29	94	412
	3	1650	0.70	430	0.95	1.36	1.78	2.88	0.35	254	411
	4	2446	2.71	435	3.47	1.28	13.95	0.82	0.20	515	30
		2488	2.75	434	1.67	0.61	16.17	1.05	0.09	588	38
		2492	2.10	432	1.56	0.74	11.76	1.01	0.12	560	48
		2516	1.87	435	1.64	0.88	10.41	0.84	0.14	557	45
		2518	1.83	436	1.76	0.96	10.01	0.88	0.15	547	48
		2524	2.19	433	2.02	0.92	11.53	1.01	0.15	526	46
		2534	2.54	433	3.45	1.36	12.98	1.22	0.21	511	48
		2536	2.80	433	2.97	1.06	14.17	1.37	0.17	506	49
		2544	3.77	431	3.20	0.85	19.62	1.05	0.14	520	28
		2548	4.38	436	2.86	0.65	25.21	0.93	0.10	576	21
		2550	3.66	436	2.46	0.67	19.72	0.97	0.11	539	27
		2564	1.28	437	2.06	1.61	4.88	1.12	0.30	381	88
		2566	3.13	436	2.67	0.85	16.11	0.95	0.14	515	30
		2568	2.98	436	2.57	0.86	15.20	0.97	0.14	510	33
		2570	2.06	435	2.71	1.32	9.55	0.92	0.22	464	45
		2572	4.13	438	3.31	0.80	23.06	0.84	0.13	558	20
		2572	6.45	436	4.40	0.68	38.26	0.90	0.10	593	14
		2574	5.57	430	4.32	0.78	33.19	0.87	0.12	596	16
	5	1555	0.33	419	0.05	0.15	0.11	1.09	0.33	33	330
	6	1408	1.89	412	5.23	2.77	6.08	2.12	0.46	322	112
		1612	0.16	418	0.13	0.81	0.24	0.34	0.35	150	213
		1658	0.33	420	0.31	0.94	0.71	0.62	0.30	215	188
		1710	0.08	347	0.11	1.38	0.10	0.24	0.52	125	300
		1311	3.28	411	0.45	0.14	22.18	2.02	0.02	676	62
		1348	1.67	413	0.51	0.31	9.70	2.10	0.05	581	126
		1378	7.13	410	1.94	0.27	49.86	3.17	0.04	699	44
		1394	4.03	409	1.16	0.29	26.57	3.31	0.04	659	82
		1414	2.40	410	0.62	0.26	15.43	2.58	0.04	643	108
	7	2121	1.37	422	0.41	0.30	7.98	0.53	0.05	582	39
		2137	2.68	424	1.19	0.44	16.94	0.70	0.07	632	26
	8	1100	0.08	418	0.10	1.25	0.26	0.50	0.28	325	625
		1130	0.11	427	0.09	0.82	0.15	0.76	0.38	136	691
		1035	0.48	406	0.31	0.65	0.29	3.13	0.51	60	652
		1040	0.62	378	0.42	0.68	1.54	3.22	0.21	248	519
	9	1862	1.49	419	3.99	2.68	2.26	2.97	0.64	152	199
	10	1756	6.54	410	3.37	0.52	36.64	2.24	0.08	560	34

Block	Well	Depth(m)	TOC	T_{MAX}(°C)	S1	S1/TOC	S2	S3	PI	HI	OI
B and C	11	2131	1.08	415	2.85	2.64	1.23	1.08	0.70	114	100
		2137	0.75	394	1.56	2.08	0.85	1.65	0.65	113	220
		2173	0.37	422	0.65	1.76	0.87	1.16	0.43	235	314
		2182	1.28	414	0.93	0.73	5.06	1.34	0.16	395	105
		2188	1.35	421	1.12	0.83	4.49	1.59	0.20	333	118
		2201	1.16	424	1.05	0.91	4.23	1.79	0.20	365	154
	12	930	0.83	421	2.61	3.14	0.38	1.79	0.87	46	216
		1056	0.25	**	0.12	0.48	0.04	1.35	0.75	16	540
		1058	0.30	406	0.10	0.33	0.13	1.69	0.44	43	563
		1060	0.54	427	0.17	0.31	0.40	1.70	0.30	74	315
		1062	0.48	419	0.22	0.46	0.22	1.85	0.50	46	385
		1064	0.32	409	0.12	0.38	0.02	1.52	0.86	6	475
		1072	0.40	416	0.11	0.28	0.05	1.51	0.69	13	378
		1094	0.51	404	0.11	0.22	0.12	1.60	0.47	24	314
		1106	0.51	431	0.18	0.35	0.92	0.63	0.16	180	124
		1108	0.43	428	0.20	0.47	0.69	0.72	0.23	160	167
		1110	0.39	433	0.21	0.54	0.57	0.66	0.27	146	169
	13	1846	0.30	**	0.11	0.37	0.21	1.58	0.34	70	527
		1890	0.29	411	0.14	0.48	0.33	1.28	0.29	114	441
D	14	3539	0.17	441	0.26	1.53	0.20	0.63	0.57	118	371
		3619	0.31	440	0.29	0.94	0.66	0.19	0.31	213	60
		3695	0.10	451	0.19	1.90	0.09	0.32	0.68	90	320
		3790	0.24	440	0.91	3.79	0.40	0.27	0.69	167	112
	15	2551	0.87	436	2.58	2.97	3.96	1.33	0.39	455	153
		2615	1.11	430	3.89	3.50	3.20	1.18	0.55	288	106
	16	3578	0.38	430	0.41	1.08	1.03	0.70	0.28	271	184
		3674	0.15	425	0.26	1.73	0.07	0.67	0.79	47	447
		3778	0.13	426	0.27	2.08	0.00	0.72	1.00	0	554
		3852	0.22	428	0.55	2.50	0.22	0.75	0.71	100	341
	17	2260	0.44	432	0.14	0.32	0.32	1.11	0.30	73	252
		2380	0.38	435	0.16	0.42	0.52	0.73	0.24	138	193
		2420	3.86	421	0.96	0.25	14.16	2.73	0.06	367	71
		2450	1.34	425	0.35	0.26	5.42	1.16	0.06	404	87
		2480	0.43	432	0.12	0.28	0.47	0.66	0.20	110	154
		2490	0.98	435	0.16	0.16	1.11	1.21	0.13	113	124
E	18	3550	1.13	429	0.58	0.51	5.16	0.66	0.10	457	58

Peters and Cassa [26] presented standard guidelines for evaluating organic richness, quality, and maturity of source rock based on pyrolysis parameters in which a TOC value of 0.5 wt.% is considered as the base limit for an effective source rock. Based on this standard, the TOC range of middle Sarvak formation exhibits variable changes with a lateral alteration in the depositional environment conditions.

The middle Sarvak formation in block A from the eastern Persian Gulf area has a TOC content of 0.08-7.13 wt.%. These values are consistent with source rocks that may have poor to excellent source rock potential with S2 ranging from 0.1 to 49 (mg HC)/(g. rock) at an average S2 value of 12 (mg HC)/(g. rock) [27]. B and C block in the central part of the study area has a TOC content of 0.25-1.35 wt.%. The middle Sarvak formation in this area represents a poor to fair hydrocarbon potential with respect to organic concentration. Moving to the western part (block D), it becomes evident that the middle Sarvak formation in this area is fair to good in terms of oil generation potential (TOC content of 0.1-3.86 wt.% with an average value of 0.69 and an S2 of 0.07-14.16 (mg HC)/(g. rock) at an average S2 value of 2.11 (mg HC)/(g. rock)) (Table 1). Source rock potentiality of middle Sarvak formation was also estimated from the HI versus TOC and S1+S2 versus TOC plots from the Rock-Eval pyrolysis output. These plots indicate variable source rock quality for the middle Sarvak formation in the sampled areas. According to this figure, the data points representing samples from block B and C indicate poor to fair source quality. Poor to excellent oil source quality is represented for Blocks A and D located in the northwest (Figure 5 and Figure 6). As a result, in the regional context, TOC and source rock potentiality variation of the middle Sarvak formation are in satisfactory agreement with the Persian Gulf basin morphology. As represented in the map of Figure 2, Qatar-Fars Arc played an important role in deposition and preservation of organic matter. Qatar-Fars Arc Paleo-high divided the Persian Gulf basin into two distinct basins, namely one in the west and another in the east of Qatar-Fars Arc. The amounts of TOC increase from central Persian Gulf towards northwestern direction in the western basin and northeast direction in the eastern basin.

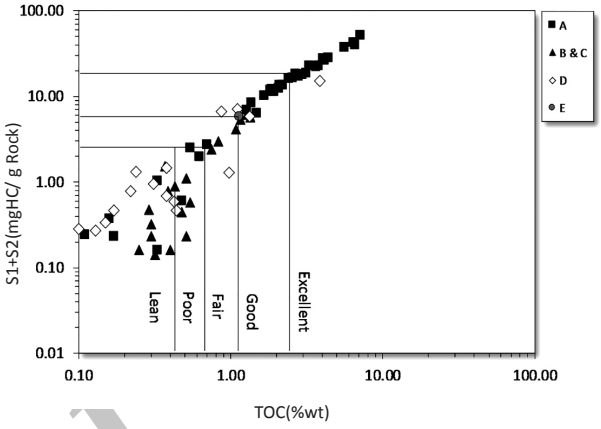

Figure 5: S1+S2 versus TOC in the middle Sarvak formation [27].

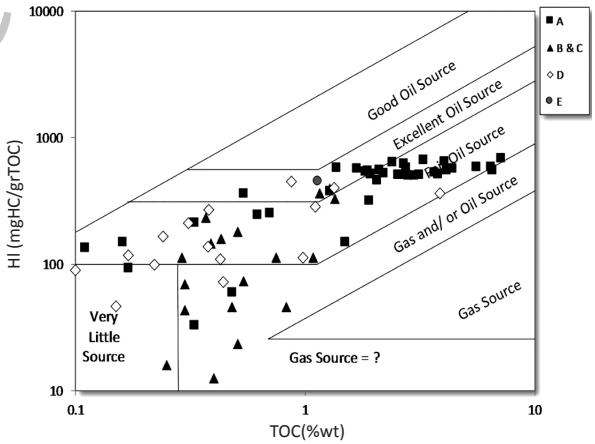

Figure 6: HI versus TOC in the middle Sarvak formation [27].

Kerogen Type

The type of organic matter present in the source rocks can be evaluated based on the plot of S2 (remaining hydrocarbon potentiality) verses TOC and modified Van Krevelen diagrams of HI versus temperature of maximum generation (Tmax) and OI versus HI. In the modified Van Krevelen diagram of HI-OI and HI-Tmax and S2 versus TOC (Figure 7, Figure 8, and Figure 9),

most of the studied samples fall in the zone of Type II and mixed Types II-III kerogen. Mixed Type II/III kerogen may originate from the mixtures of terrigenous and marine organic matter with varying oil and gas generation potentials. This type of organic matter may also originally be marine Type II organic matter, which has partially been oxidized during deposition. Additional support is provided by the chemical and optical studies of the organic matter. These methods provide better means for defining the type of organic matter in the studied samples. The optical analysis of organic matter was conducted on selected samples from both D and A blocks. These results revealed that liptinite is the major maceral constituent inside the middle Sarvak formation (Figure 10). This result is in agreement with the higher amounts of amorphous particles in the studied samples under transmitted light. The elemental analysis data, in combination with the Rock-Eval data, support the optical methods result. All of the studied sample have higher amounts of elemental hydrogen (and similarly higher HI values), implying that a major proportion of the organic matter available in the studied samples is of Type II (Table 2). The results from the elemental analysis of selected samples are displayed in a typical Van Krevelen diagram by plotting H/C versus O/C ratios. Figure 11 shows the Van Krevelen cross-plot for the organic matter of the analyzed samples. The occurrence of uplift in the central part of the Persian Gulf resulted from the presence of the Qatar Arch provided a shallower sea in this part of the study area. Consequently, organic matters were exposed to more oxidizing activities resulting in relatively poor preservation of organic matter in the central Persian Gulf compared to the other parts. As a result, the organic matter quality of middle Sarvak formation shows an increase in the potentiality of sedimentary environment for organic matter accumulation and preservation by moving from central part (block B and C) to the west (block D) and east (block A) part of the Persian Gulf.

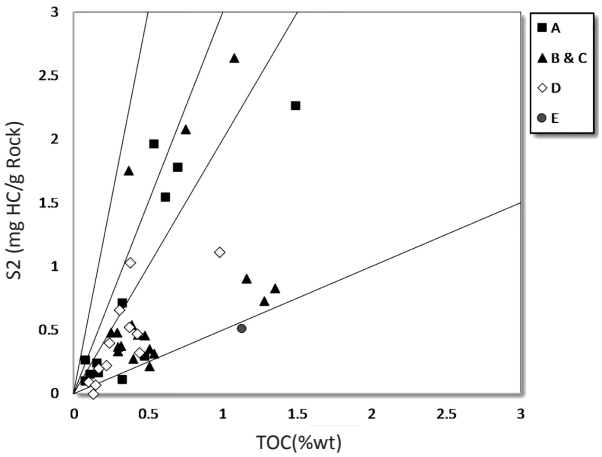

Figure 7: S2 versus TOC in middle Sarvak [29].

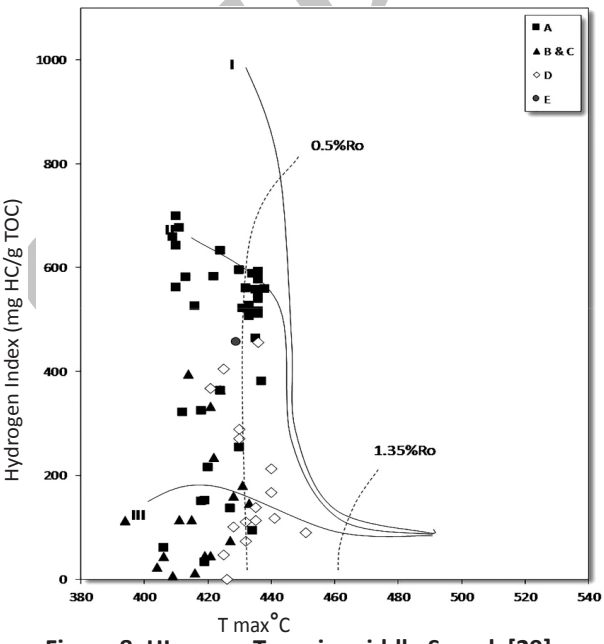

Figure 8: HI versus Tmax in middle Sarvak [29].

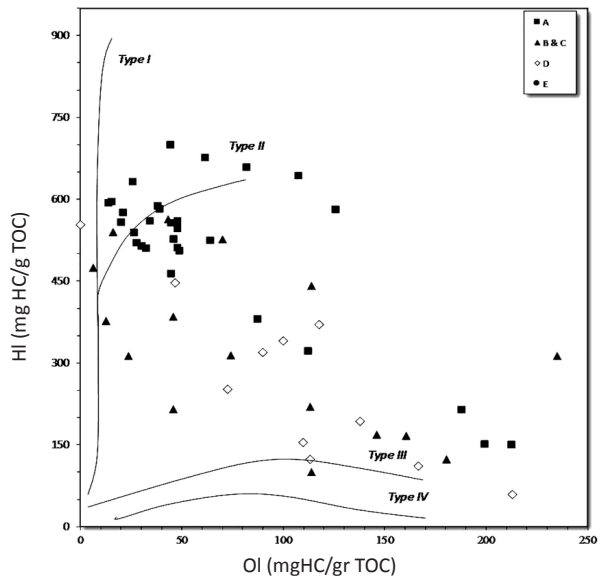

Figure 9: HI versus OI in middle Sarvak [29].

Table 2: Determination of kerogen type based on chemical and optical properties of middle Sarvak formation.

General Information Elemental Analyze			Chemical methods				Optical Methods							
			Rock-Eval		Reflected Light		Transmitted Light							
Block	Well	Sample No. Interval	H/C	O/C	HI	OI	Vit.	Lip.	Iner.	Amor.	Herb.	Woody	Coaly	Kerogen Type
D	7	S-1034-1035	1.13	0.17	386	79	30	50	20	65	0	15	20	II
A	4	S-637-638	1.3	0.03	595	15	30	60	10	75	5	10	10	II
A	4	S-645	1.4	0.03	576	21	30	50	20	80	0	15	5	II
A	4	S-653-654	1.23	0.05	551	34	35	60	5	70	0	20	10	II
A	6	S-75-79	1.32	0.11	655	84	30	60	20	85	0	5	10	II
A	6	S-81-86	1.2	0.14	672	71	20	65	15	80	0	10	10	II
Average			1.3	0.1	572.4	50.7	29	58	15	76	1	13	11	

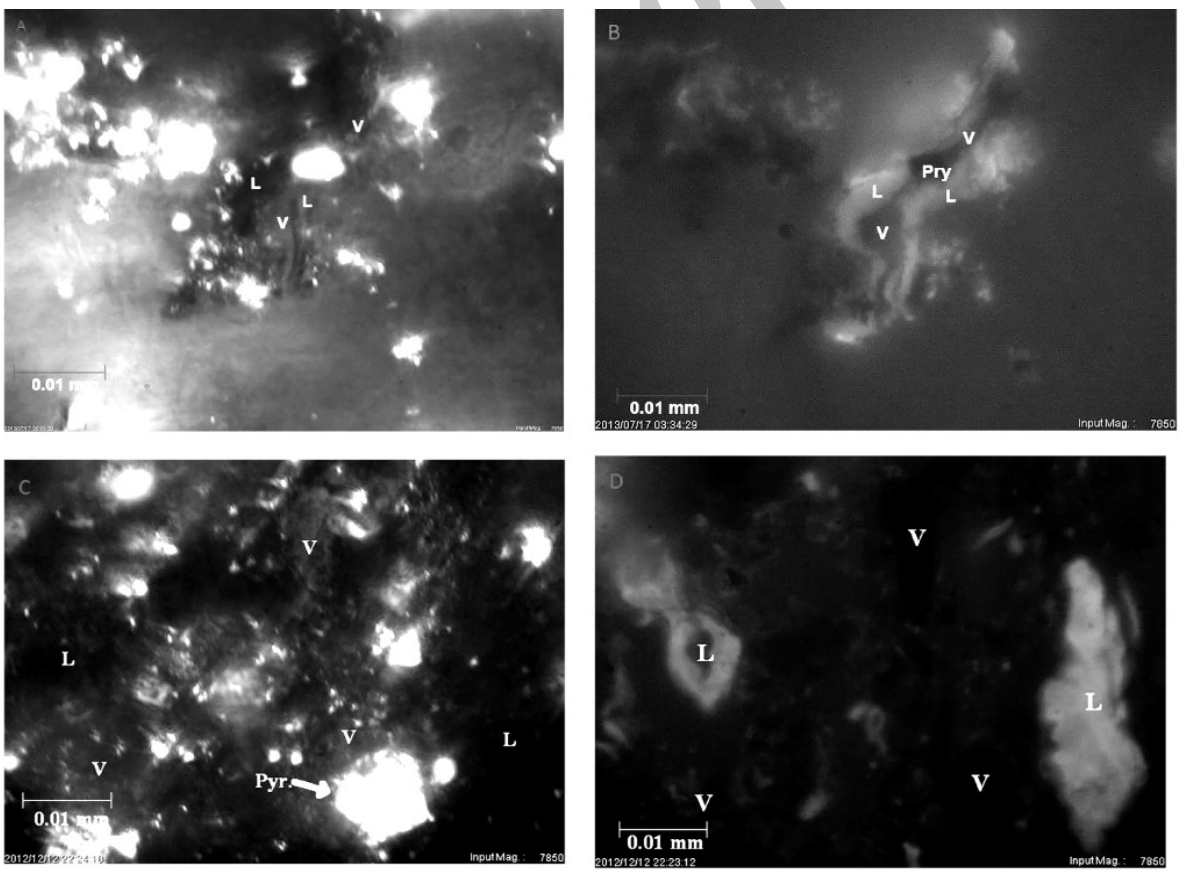

Figure 10: Photomicrographs of macerals in the middle Sarvak formation; A and C are reflected light, and B and D are UV; (V: Vitrinite, L: Liptinite).

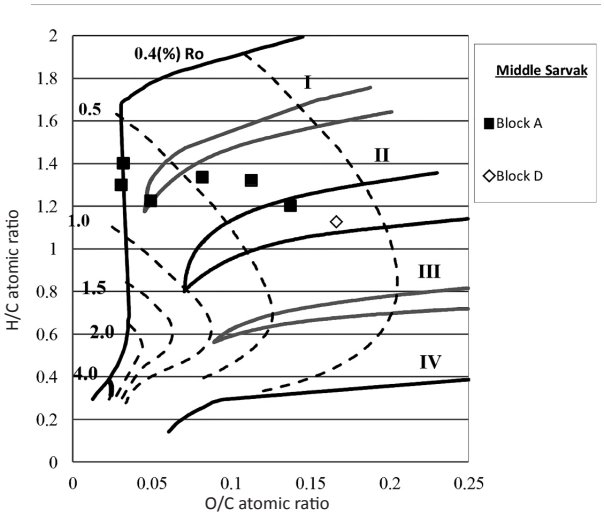

Figure 11: Bivariate plot H/C versus O/C for middle Sarvak formation [30].

Organic Matter Thermal Maturity

The level of maturity is evaluated using two main factors, including petrographical observation and thermal indicators. Vitrinite reflectance and palynofacies analysis are the most reliable petrographical indicators. Meanwhile, Tmax obtained from Rock-Eval pyrolysis, is a good thermal indicator of organic maturity [29, 28]. The extent of organic maturation of the middle Sarvak formation was evaluated by using several important parameters. Tmax and production index (PI) were used for this purpose. In addition, petrographic data such as vitrinite reflectance measurements and thermal coloration studies (both fluorescence and transmitted light microscopy) were applied. The bottom of oil generation is considered to be equivalent as a vitrinite reflectance of 0.6% (Tmax =435 °C), and its peak is regarded to be around 0.65-0.9% VRo (Tmax ranges from 445 °C to 450 °C) [26].

The plot of Tmax versus HI for 4 blocks over the study area illustrates different levels of maturity for middle Sarvak formation (Figure 8). As shown in this figure and Table 1, samples obtained from block A in the eastern part of Persian Gulf have a Tmax value ranges between 406 and 438 °C with an average value of 425 °C. This evidence indicates that the middle Sarvak formation in block A is located at early oil generation window. Meanwhile, the level of maturity considerably decreased according to Figure 8, moving towards central part. In block B and C from the central part of the Persian Gulf, Tmax ranges from 394 °C to 433 °C with an average value of 417 °C. Regarding Peters's classification [26], the middle Sarvak formation in this area falls within immature zone and could not produce commercial gas and liquid hydrocarbons. In block D, the western part of the study area, Tmax value ranges between 421 °C and 451 °C with an average value of 435 °C, which means the middle Sarvak formation is located in the early stage of oil window maturation level.

The level of organic matter maturity was also estimated from the Tmax versus PI plot from the Rock-Eval pyrolysis output [28]. According to this diagram, Tmax of oil generation zone ranges between 435 °C and 460 °C, and its PI values lie between 0.1 and 0.4. The average PI value for the middle Sarvak formation varies in different blocks in the study area (Figure 12 and Figure 13). These figures indicate that this formation is thermally mature in block A and D and is placed in a nearly hydrocarbon generation zone. However, the middle Sarvak formation in block B and C from the central part of the Persian Gulf is not located in the hydrocarbon generation zone. Meanwhile, these figures (Figure 12 and Figure 13) can be used to identify the type of hydrocarbon produced. According to these relations, the samples from block B and C are thermally immature, and the hydrocarbons are nonindigenous; nevertheless, in A and D blocks, samples are nearly thermally mature, and the hydrocarbons are considered to be most indigenous (PI ranges from 0.1 to 0.4).

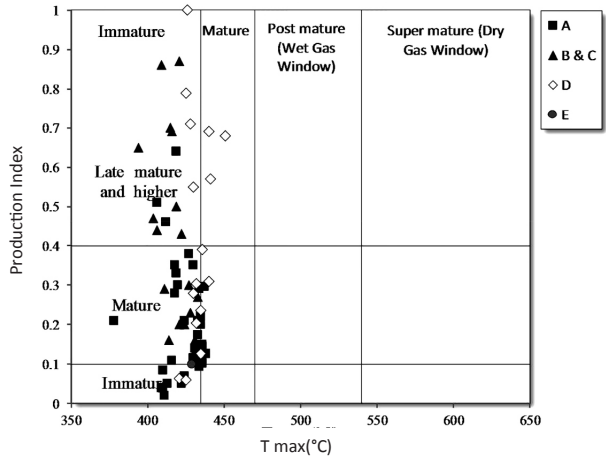

Figure 12: PI versus Tmax diagram in middle Sarvak formation [31].

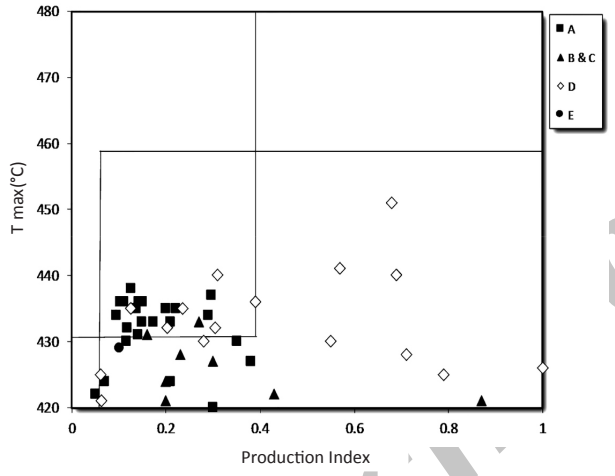

Figure 13: Tmax versus PI diagram in middle Sarvak formation [32].

The maturity of the middle Sarvak formation is also evaluated by using vitrinite reflectance measurements. Vitrinite reflectance data for the studied formation over the Persian Gulf area is shown in Table 3. The range of vitrinite reflectance data in the middle Sarvak formation is between 0.45% and 0.6% in Block A, with an average value of 0.52%, which means this formation located in the early stage of oil generation window. In Block D, vitrinite reflectance data ranges from 0.51% to 0.57 % with an average of 0.54%. This parameter indicates that the middle Sarvak formation in the western part of the Persian Gulf falls within the oil window maturation level. Meanwhile, the level of maturity considerably decreased, according to VRo data, by moving from east (block A) and west part (block D) towards the central part (block B and C) of the Persian Gulf. In block B and C, vitrinite reflectance data range from 0.36% to 0.44%, averaging 0.4%, which means that the middle Sarvak formation in this area falls within an immature zone and could not produce commercial gas and liquid hydrocarbons. Iso-reflectance map for this formation based on 18 measurements over the study area is shown in Figure 14. According to this figure, it can be concluded that the middle Sarvak formation has remained immature in the central parts, but it has reached the oil generation stage in the western and eastern parts of the Persian Gulf. The comparison between VRo map and burial depth map of the formation (Figure 15) illustrates a good correlation between these two parameters, which indicates a role of burial depth in the thermal maturity of the formation. The burial depth of the middle Sarvak formation is an important variable which is considered to affect geologically related properties such as thermal maturity (Figure 15). The figure proposes an increase in the central parts of the study area (Qatar-Fars Arc) toward the western and eastern parts (from about less than 1000 m to more than 3000 m). The thickest zones (blocks A and D) represent more accommodation space (i.e. deeper basins). Accordingly, trough zones are more susceptible to the maturation of the middle Sarvak formation, which is in agreement with the thermal indicator spatial variation in the Persian Gulf area. Thermal alteration index (TAI) measured based on the kerogen color is also consistent with these findings. In this study, the color of the organic matter inside the middle Sarvak formation varies from light brown to medium brown (Figure 16) with corresponding TAI values ranging from 2 to 2+ (Table 4). Generally, these results show an immature to early mature zone for the studied samples.

Table 3: Vitrinite reflectance data (Ro%) of the Sarvak formation in the Persian Gulf.

Block	Well	Formation	Sample No.	Depth	Number of Reading	Vitrinite Reflectance (%)		
						Min	Max	Mean
B and C	11	Middle Sarvak	FC-1-17	2130.55	5	0.3	0.66	0.44
B and C	11	Middle Sarvak	FC-1-19	2173.22	5	0.33	0.57	0.40
B and C	11	Middle Sarvak	FC-1-22	2200.66	3	0.27	0.53	0.38
A	2	Middle Sarvak	S-587	1329	11	0.36	0.54	0.46
A	4	Middle Sarvak	S-654	2446	16	0.46	0.69	0.54
A	4	Middle Sarvak	S-653	2488	8	0.42	0.62	0.53
A	4	Middle Sarvak	S-652	2492	8	0.43	0.63	0.52
A	4	Middle Sarvak	S-649	2524	11	0.44	0.62	0.54
A	4	Middle Sarvak	S-647	2536	10	0.45	0.62	0.52
A	4	Middle Sarvak	S-645	2548	10	0.48	0.67	0.55
A	4	Middle Sarvak	S-644	2550	9	0.48	0.65	0.55
A	4	Middle Sarvak	S-641	2568	11	0.47	0.71	0.57
A	4	Middle Sarvak	S-639	2572	10	0.47	0.71	0.6
A	4	Middle Sarvak	S-637	2574	11	0.46	0.72	0.6
B and C	13	Middle Sarvak	S-911	1846	9	0.31	0.43	0.36
D	17	Middle Sarvak	S-1037	2260	14	0.43	0.6	0.51
D	17	Middle Sarvak	S-1035	2420	8	0.47	0.68	0.55
D	17	Middle Sarvak	S-1034	2450	11	0.48	0.7	0.56
D	17	Middle Sarvak	S-1032	2490	13	0.48	0.7	0.57

Table 4: Range and mean of Ro% and TAI data for the middle Sarvak formation in different blocks.

Block	Number of Samples	Range of Ro	Average Ro (%)	TAI	Maturity
A	11	0.46-0.6	0.54	+2 to 2	Early Mature
B and C	4	0.36-0.44	0.39	-	Immature
D	4	0.51-0.57	0.54	+2	Early Mature
E	No sample	-	-	-	-

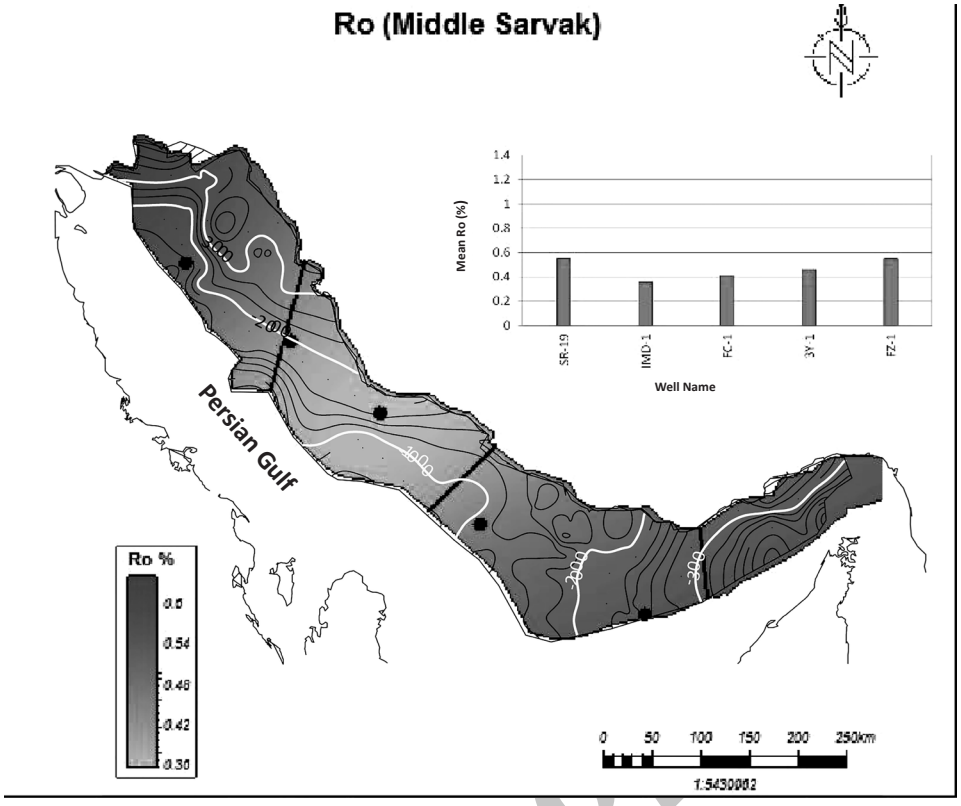

Figure 14: Regional variation of Ro data for the middle Sarvak formation in the Persian Gulf.

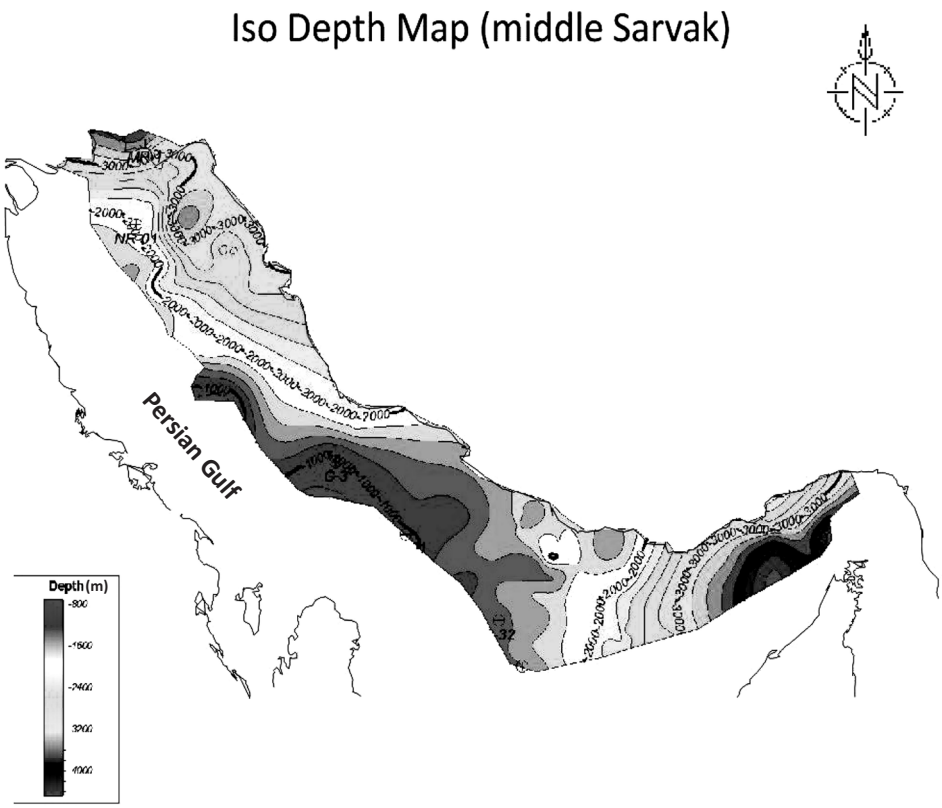

Figure 15: Depth map of the middle Sarvak formation; Qatar-Fars Arc Paleo-high represents the minimum depth for the middle Sarvak formation.

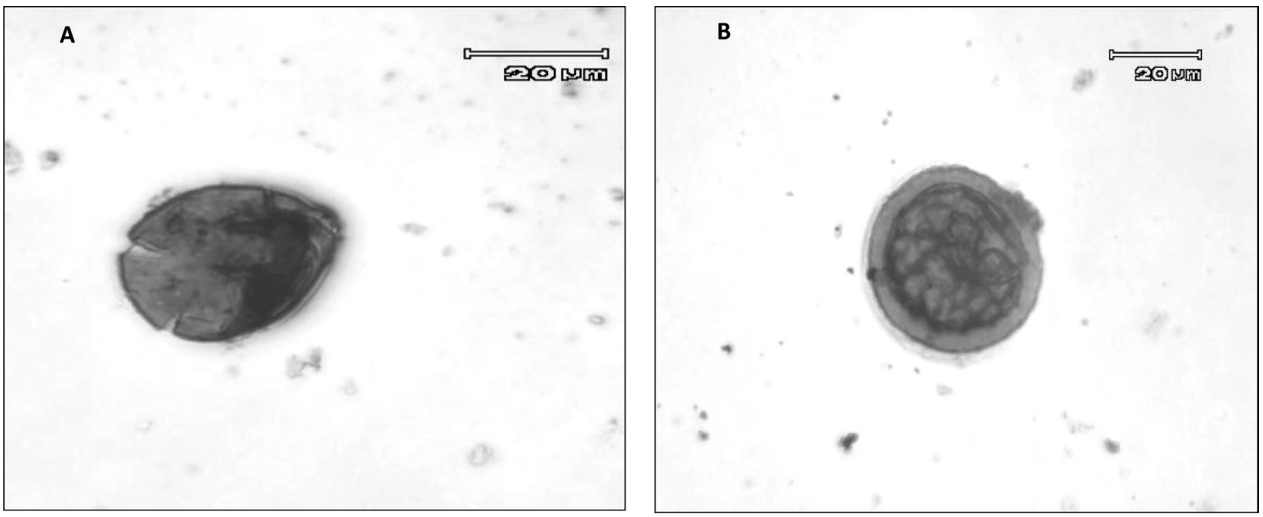

Figure 16: Organic matter of the middle Sarvak formation under transmitted light.

CONCLUSIONS

In this study, the source rock potential of 76 cutting samples from the middle Sarvak formation in the Persian Gulf were investigated. This investigation was based on the gathered data such as source rock richness, quality, distribution, and maturity which were obtained from Rock-Eval, vitrinite reflectance, and palynofacies analyses.

In summary, based on the Rock-Eval pyrolysis results, the variation of organic matter quality- and quantity-dependent parameters indicates Type II/III kerogen in the western and eastern blocks (A and D) and Type III kerogen in block B and C . The result of this study shows that middle Sarvak formation is immature in the central area of the Persian Gulf. The existence of Qatar-Fars Arc causes uplift in this region and can be a reason for immaturity in this part of the study area. In contrast to the central part, the middle Sarvak formation has entered to oil window in the eastern and western areas. The overall asymmetric nature of the basin in combination with shallower basement in the central parts with respect to the eastern and western regions resulted in the different trend of maturity in the study area. The higher maturity in the eastern and western regions can be attributed to the increasing burial depth and thickness of this formation toward the northwest and east.

ACKNOWLEDGMENTS

This work was conducted as a part of Pearl Program Research which is shared project between Iranian Offshore Oil Company (IOOC) and RIPI. The authors gratefully acknowledge Iranian Offshore Oil Company IOOC staff, especially Dr. Ali Chehrazi for the financial support of the project. Also, we appreciate Prof. Kotarba for assistance with the Rock Eval pyrolysis at RIPI and AGH university of Poland respectively.

REFERENCES

1. Ghazban F., "Petroleum Geology of the Persian Gulf," Tehran University, **2007**.
2. Bordenave M. L. and Burwood R., "Source Rock Distribution and Maturation in the Zagros Orogenic Belt: Provenance of the Asmari and Bangestan Reservoir Oil Accumulations," *Organic Geochemistry*, **1990**, *16*(1), 369-387.
3. Bordenave M. L. and Huc A. Y., "The Cretaceous Source Rocks in the Zagros Foothills of Iran: An Example of a Large Size Intracratonic Basin," *AAPG Bulletin*. 77. CONF-930306, **1993**.
4. Bordenave M. L. "The Middle Cretaceous to Early Miocene Petroleum System in the Zagros Domain of Iran, and its Prospect Evaluation," *AAPG Annual*

Meeting, Houston, Texas, **2002**.

5. Beiranvand B., Ahmad. A., and Sharafodin M., "Mapping and Classifying Flow Units in the Upper Part of the Mid-cretaceous Sarvak Formation (Western Dezful Embayment, SW Iran) Based on a Determination of Reservoir Rock Types," *Journal of Petroleum Geology,* **2007**, *30*(4), 357-373.
6. Kent P., "The Emergent Hormuz Salt Plugs of Southern Iran," *Journal of Petroleum Geology,* **1979**, *2*, 117-144.
7. Murris R. J., "Middle East-Stratigraphic Evolution and Oil Habitat," *ABSTRACT. AAPG Bulletin*, **1981**, *65*, 1358-1358.
8. Alsharhan A., "Oxfordian-Kimmeridgian Diyab Formation as a Major Source Rock Unit in Southern Arabian Gulf," *The Society for Organic Petrology (TSOP)*, 18th Annual Meeting, **2001**
9. Alsharhan A. and Magara, K., "The Jurassic of the Arabian Gulf Basin: Facies, Depositional Setting and Hydrocarbon Habitat," *Global Environments and Resources*, **1994**, *17*, 397-412.
10. Lasemi Y. and Jalilian A., "The Middle Jurassic Basinal Deposits of the Surmeh Formation in the Central Zagros Mountains, Southwest Iran: Facies, Sequence Stratigraphy, and Controls," *Carbonates and Evaporites*, **2010**, *25*(4), 283-295.
11. Alsharhan A. and Kendall C. S. C., "Cretaceous Chronostratigraphy, Unconformities and Eustatic Sea Level Changes in the Sediments of Abu Dhabi, United Arab Emirates," *Cretaceous Research*, **1991**, *12*, 379-401.
12. Van Buchem F. S., Razin P., Homewood P. W., Oterdoom W. H., and Philip J., "Stratigraphic Organization of Carbonate Ramps and Organic-rich Intrashelf Basins: Natih Formation (Middle Cretaceous) of Northern Oman," *AAPG Bulletin,* **2002**, *86*, 21-53.
13. Vincent B., van Buchem F. S., Bulot L. G., Jalali M., et al., "Depositional Sequences, Diagenesis and Structural Control of the Albian to Turonian Carbonate Platform Systems in Coastal Fars (SW Iran)," *Marine and Petroleum Geology,* **2015**, *63*, 46-67.
14. Alsharhan A. and Nairn A., "Carbonate Platform Models of Arabian Cretaceous Reservoirs," *AAPG Special Publications*, **1993**, 56, 173-184.
15. Faqira M., Rademakers M., and Afifi A., "New Insights into the Hercynian Orogeny, and their Implications for the Paleozoic Hydrocarbon System in the Arabian Plate," *GeoArabia*, **2009**, *14*, 199-228.
16. Soleimany B., Nalpas T. i., and Montserrat F. S., "Multidetachment Analogue Models of Fold Reactivation in Transpression: the NW Persian Gulf," *Geologica Acta: an International Earth Science Journal*, **2013**, *11*, 265-276.
17. Jordan J. r., Connolly J. r., and Vest H. A., "Middle Cretaceous Carbonates of the Mishrif Formation, Fateh Field, Offshore Dubai, UAE," Carbonate Petroleum Reservoirs, *Springer*, **1985**, 425-442.
18. Aali J., Rahimpour-Bonab H. and Kamali M. R., "Geochemistry and Origin of the Worlds Largest Gas Field from Persian Gulf, Iran," *Journal of Petroleum Science and Engineering*, **2006**, *50*, 161-175.
19. Ziegler M. A., "Late Permian to Holocene Palynofacies Evolution of the Arabian Plate and its Hydrocarbon Occurrences," *Journal of Geoarabia*, **2001**, *6*, 445-504.
20. Perotti C. R., Bertozzi G., Feltre L., Rahimi M., et al., "The Qatar-South Fars Arch Development (Arabian Platform, Persian Gulf): Insights from Seismic Interpretation and Analogue Modelling," INTECH Open Access Publisher, **2011**.
21. Ghazban F. and Al-Aasm I. S., "Hydrocarbon-induced Diagenetic Dolomite and Pyrite

Formation Associated with the Hormoz Island Salt Dome, Offshore Iran," *Journal of Petroleum Geology*, **2010**, *33*, 183-196.

22. Mashhadi Z. S., Rabbani A. R., Kamali M. R., Mirshahani M., et al., "Burial and Thermal Maturity Modeling of the Middle Cretaceous–Early Miocene Petroleum System, Iranian Sector of the Persian Gulf," *Petroleum Science*, **2015**, *12*, 367-390.
23. Sharland P. R., Archer R., Casey D., Davies,R., et al., "Arabian Plate Sequence Stratigraphy," *GeoArabia, Journal of the Middle East Petroleum Geosciences,* **2013**, *18*, 56-74.
24. Mina P., Razaghnia M. T. , and ParanY., "Geological and geophysical studies and exploratory drilling of the Iranian continental shelf–Persian Gulf," *7th World Petroleum Congress*, World Petroleum Congress, **1967**.
25. Taylor G. H., "Organic Petrology: Berlin," *Gebrüder Borntraeger*, **1998**.
26. Peters K. E. and Cassa M. R., "Applied Source Rock Geochemistry," Chapter 5: Part II, *Essential Elements*, **1994**, 93-120.
27. Kenneth E. P., Walters C. C., and Moldowan J. M., "The Biomarker Guide: Biomarkers and Isotopes in the Environment and Human History," Cambridge University Press, **2005**.
28. Hunt J. M., "Petroleum Geology and Geochemistry," Freeman and Company, New York, **1996**.
29. Krevelen D. W., "Coal-typology, Chemistry, Physics, Constitution," *Elsevier Science and Technology*, *3*, **1961**.
30. Magoon L. B. and Wallace G. D., "The Petroleum System-from Source to Trap," *AAPG Memoir*, **1994**, *60*, 3-24.
31. Langford F. F. and Blanc-Valleron M. M., "Interpreting Rock-Eval Pyrolysis Data Using Graphs of Pyrolizable Hydrocarbons vs. Total Organic Carbon," *AAPG Bulletin,* **1990**, *74*(6), 799-804.